



# HHS Public Access

Author manuscript

*Br J Haematol.* Author manuscript; available in PMC 2021 February 03.

Published in final edited form as:

*Br J Haematol.* 2021 February ; 192(3): 652–663. doi:10.1111/bjh.17230.

## FANCD2 and HES1 suppress inflammation-induced PPAR<sub>γ</sub> to prevent haematopoietic stem cell exhaustion

Limei Wu<sup>1</sup>, Xue Li<sup>1</sup>, Qiqi Lin<sup>1</sup>, Fabliha Chowdhury<sup>1</sup>, Md H. Mazumder<sup>1</sup>, Wei Du<sup>1,2,3,4</sup>

<sup>1</sup>Department of Pharmaceutical Sciences, School of Pharmacy, West Virginia University

<sup>2</sup>Alexander B. Osborn Hematopoietic Malignancy and Transplantation Program, West Virginia University Cancer Institute, Morgantown, WV

<sup>3</sup>Division of Hematology and Oncology, University of Pittsburgh School of Medicine

<sup>4</sup>Genome Stability Program, UPMC Hillman Cancer Center, Pittsburgh, PA, USA

### Summary

The Fanconi anaemia protein FANCD2 suppresses PPAR<sub>γ</sub> to maintain haematopoietic stem cell's (HSC) function; however, the underlying mechanism is not known. Here we show that FANCD2 acts in concert with the Notch target HES1 to suppress inflammation-induced PPAR<sub>γ</sub> in HSC maintenance. Loss of *HES1* exacerbates *FANCD2*-KO HSC defects. However, deletion of *HES1* does not cause more severe inflammation-mediated HSC defects in *FANCD2*-KO mice, indicating that both FANCD2 and HES1 are required for limiting detrimental effects of inflammation on HSCs. Further analysis shows that both FANCD2 and HES1 are required for transcriptional repression of inflammation-activated *PPARg* promoter. Inflammation orchestrates an overlapping transcriptional programme in HSPCs deficient for *FANCD2* and *HES1*, featuring upregulation of genes in fatty acid oxidation (FAO) and oxidative phosphorylation. Loss of *FANCD2* or *HES1* augments both basal and inflammation-primed FAO. Targeted inhibition of PPAR<sub>γ</sub> or the mitochondrial carnitine palmitoyltransferase-1 (CPT1) reduces FAO and ameliorates HSC defects in inflammation-primed HSPCs deleted for *FANCD2* or *HES1* or both. Finally, depletion of *PPARg* or *CPT1* restores quiescence in these mutant HSCs under inflammatory stress. Our results suggest that this novel FANCD2/HES1/PPAR<sub>γ</sub> axis may constitute a key component of immunometabolic regulation, connecting inflammation, cellular metabolism and HSC function.

### Keywords

bone marrow transplant; fatty acid oxidation; haematopoietic stem and progenitor cells; inflammation; PPAR<sub>γ</sub>; stem cell quiescence

Correspondence: Wei Du, Division of Hematology and Oncology, University of Pittsburgh School of Medicine, Pittsburgh, PA 15213, USA. duw@upmc.edu.

Author contributions

LW performed the research and analyzed the data; XL, QL, FAC and MHHM performed some of the research and assisted in data analysis. WD designed the research, analyzed the data, and wrote the paper.

Conflicts of interest

The authors declare no conflicts of interest.

Supporting Information

Additional supporting information may be found online in the Supporting Information section at the end of the article.

## Introduction

Fanconi anaemia (FA) is a genetic disorder associated with bone marrow failure (BMF), developmental defects, metabolic disorder and cancers, particularly leukaemia,<sup>1</sup> (Schneider *et al.*, 2015).<sup>2</sup> It is genetically heterogeneous, with at least 22 complementation groups (*FANCA–FANCW*) identified thus far. At the molecular level, a DNA damage repair-based FA pathway has been established.<sup>3,4</sup> Haematopoietic stem cell (HSC) failure is now considered the root cause of FA BMF and leukaemia. *FA* gene deficiency in patients as well as knockout mice results in severe reduction of HSC both in quantity and quality.<sup>4,5-8</sup> HSCs from mice deficient for several *FA* genes exhibit profound haematopoietic repopulating defects in irradiated transplanted recipients.<sup>8-11</sup> Furthermore, *ex vivo* culture of BM cells deficient for the *Fancc* gene leads to an increase in cytogenetic abnormalities and myeloid malignancies, suggesting FA haematopoietic cells are prone to clonal haematopoiesis and malignancy.<sup>5,12,13</sup> The haematological manifestations of FA include a high incidence of myelodysplastic syndrome (MDS) and acute myeloid leukaemia (AML).<sup>14,15</sup> At the centre of the FA pathway is the FANCD2/FANCI complex, the recruitment of which to the DNA damage site is a critical step of repair.<sup>3,4</sup> Clinically, patients with *FANCD2* mutations have earlier onset and more rapid progression of haematological manifestations compared with patients with mutations in other FA complementation groups.<sup>16</sup> *Fancd2*-deficient mice exhibit multiple haematopoietic defects, including HSC and progenitor loss in early development, abnormal cell cycle status, loss of quiescence in haematopoietic stem and progenitor cells (HSPCs), and compromised functional capacity of HSCs.<sup>17</sup> Recent study has shown that FANCD2 is required for nuclear retention of stress transcriptional factor FOXO3a in HSC maintenance.<sup>10</sup> However, the mechanisms by which FANCD2 functions in haematopoiesis remains largely unknown.

The transcriptional repressor Hairy Enhancer Split 1 (HES1) is one of hairy-related basic helix–loop–helix (bHLH) family members known to be involved in regulating cell fate decisions and proliferation specifically in neural cells and bone marrow.<sup>18,19</sup> In the haematopoietic system, HES1 plays major role in normal T cells development.<sup>20-22</sup> However, studies in *HES1*-deficient mice show no overt haematopoietic abnormalities in the steady state.<sup>20</sup> Overexpression of *HES1* inhibits differentiation of bone marrow HSCs when cultured *in vitro*, increase HSC self-renewal, reduce HSC cycling, and preserve the long-term reconstitution ability of primitive haematopoietic cells.<sup>23,24</sup> We recently showed that while HES1 is dispensable for steady-state haematopoiesis, *HES1*-deficient HSCs undergo exhaustion under replicative stress in a haematopoietic lineage-specific *HES1* knockout mouse model.<sup>25</sup> The mechanism by which HES1 regulates haematopoiesis remains largely unknown.

Recent studies using metabolomics technologies have revealed that metabolic regulation plays an essential role in HSC maintenance. Metabolism provides energy and building blocks for other factors functioning at steady state and in stress haematopoiesis.<sup>26</sup> Altered metabolic energetics in HSCs affects their function and underlies the onset of many blood malignancies.<sup>27-29</sup> Nuclear receptor superfamily members, peroxisome proliferator-activated receptors (PPARs), classified into three isoforms (PPAR $\alpha$ ,  $\beta/\delta$ ,  $\gamma$ ), are important in whole-

body energy metabolism and collectively involved in fatty acid oxidation (FAO).<sup>30</sup> We previously identified PPAR<sub>γ</sub> as a negative regulator of HSC using an *in vivo* RNAi screen system, and showed that FANCD2 suppresses PPAR<sub>γ</sub> to maintain HSC function.<sup>31</sup> Another independent study also suggested that inhibition of PPAR<sub>γ</sub> improves *ex vivo* expansion of human HSCs and progenitors.<sup>32</sup> Using a haematopoietic lineage-specific *HES1* knockout mouse model (*HES1<sup>fl/fl</sup>Vav1Cre*), we recently identified a novel role for the Notch target HES1 in regulating haematopoiesis under stress by regulating PPAR<sub>γ</sub> and fatty acid metabolism pathways.<sup>25</sup> How this FANCD2/HES1/PPAR<sub>γ</sub> signaling axis influences HSC function is not known.

In this study, we found that both FANCD2 and HES1 are required for limiting detrimental effects of inflammation on HSCs. Mechanistically, FANCD2 is required for HES1-mediated transcriptional repression of the inflammation-activated PPAR<sub>γ</sub> promoter. Further, we show that loss of *FANCD2* or *HES1* augments both basal and inflammation-primed FAO, and that targeted inhibition of PPAR<sub>γ</sub> or FAO ameliorates HSC defects in *FANCD2*-deficient HSCs.

## Materials and methods

### Mice

*FANCD2*<sup>+/-</sup> mice in a C57BL/6 background were provided by Dr. Markus Grompe (Oregon Health & Sciences University).<sup>33</sup> Heterozygous *HES1* mice in a C57BL/6 background<sup>34</sup> were generated from the sperm purchased from Riken, Japan ({"type": "entrez-protein", "attrs": {"text": "CSD23160", "term\_id": "903054544", "term\_text": "CSD23160"} }RBRC06047). The *in vitro* fertilization (IVF) procedure was performed at the Transgenic Animal Core Facility at West Virginia University (WVU). Heterozygous *HES1* mice (*HES1<sup>fllox/WT</sup>*) were interbred to generate *HES1* null mice (*HES1<sup>fllox/fllox</sup>*,<sup>25</sup> or crossed with *FANCD2*<sup>+/-</sup> mice to generate *FANCD2,HES1* double knockout (DKO) mice and littermate controls. The *FANCD2-KI* mice in a 129/BL6 background expressing a dual tandem (3XFLAG and HA) tag have been previously described elsewhere.<sup>35</sup> All animals including the BoyJ recipient mice were maintained in specific pathogen-free facilities at West Virginia University. Animals were kept in accordance with the regulations prescribed by the Institutional Animal Care and Use Committees (1701005049).

For detailed experimental procedures, see Supplemental Methods.

## Results

### Loss of HES1 exacerbates FANCD2<sup>-/-</sup> HSC defects

Using a published *HES1* knockout (KO) strain,<sup>25,34</sup> we deleted the *HES1* gene in *FANCD2*-KO mice and analyzed haematopoietic cell populations in the bone marrow (BM) of WT, *FANCD2*-KO, *HES1*-KO and *FANCD2,HES1* DKO mice. We found that while BM cellularity of single KO or DKO mice was comparable to that of WT littermates (Figure S1), loss of both *FANCD2* and *HES1* caused a further reduction in the frequency of HSPCs (Lin<sup>-</sup>Sca1<sup>+</sup>c-kit<sup>+</sup>, LSK) and that of the phenotypic HSCs (Lin<sup>-</sup>Sca1<sup>+</sup>c-kit<sup>+</sup>CD48<sup>-</sup>CD150<sup>+</sup>) signaling lymphocyte activation molecule (SLAM)<sup>36</sup> compared to single KO and WT

controls (Fig 1A). We also determined the haematopoietic parameters in the peripheral blood (PB) of these mice and found that loss of *HES1* led to more severe myeloid skew in *FANCD2*-KO mice compared to the single KO mice (Fig 1B, Table I). Thus, deletion of *HES1* further reduces the HSPC pool and alters lineage differentiation in *FANCD2*-KO mice.

We next examined the haematopoietic repopulating capacity of HSCs by transplanting one million whole bone marrow cells (WBMCs) from WT, *FANCD2*-KO, *HES1*-KO and DKO mice (CD45<sup>2+</sup>), along with an equal number of WBMCs from congenic BoyJ mice (CD45<sup>1+</sup>) into each lethally irradiated BoyJ recipient.<sup>8</sup> Flow cytometry analysis demonstrated a further reduced donor-derived chimaera (CD45<sup>2+</sup>, Fig 1C) and skewed lineage differentiation (Figure S2) in the PB of the recipients transplanted with DKO cells compared to those transplanted with *FANCD2*-KO or *HES1*-KO at four weeks and 16 weeks post bone marrow transplantation (BMT). These results indicate that loss of *HES1* further reduces the repopulating ability of *FANCD2*-KO HSCs. These observations were further verified by a limiting dilution assay.<sup>25,37</sup> Poisson statistical analysis at 16 weeks post-transplantation showed an approx. twofold reduction in the frequency of competitive repopulating units (CRU) in single KO donor cells and approx. fourfold reduction in DKO donor cells, compared to WT cells (Fig 1D and Table II). Thus, loss of *HES1* leads to more severe HSC exhaustion in *FANCD2*-KO mice.

### Both FANCD2 and HES1 are required for limiting detrimental effects of inflammation on HSCs

We and others have demonstrated that inflammation in FA HSPCs plays a crucial role in FA pathophysiology.<sup>38-40</sup> Since several components of the FA pathway interacted with the Notch target *HES1*<sup>41,42</sup> and since inflammation-mediated deregulation of Notch signalling skewed HSC differentiation in FA mice,<sup>7</sup> we asked whether *FANCD2* functionally interacts with *HES1* in response inflammatory cues in HSC maintenance. We first treated BM SLAM cells isolated from WT, *FANCD2*-KO, *HES1*-KO or DKO mice with increasing doses of tumour necrosis factor-alpha (TNF- $\alpha$ ), a pro-inflammatory cytokine that can efficiently induce robust inflammatory responses in HSPCs.<sup>40,43</sup> We found that TNF- $\alpha$  treatment did not further decrease *ex vivo* self-renewal of DKO HSCs compared to either single KO HSC (Fig 2A). Interestingly, functional BMT assay revealed that TNF- $\alpha$  treatment increased short-term repopulation of single KO and DKO HSCs at four weeks post-transplant (Fig 2B). However, TNF- $\alpha$  significantly reduced long-term repopulation of these KO HSCs at 16 weeks post primary BMT and in secondary recipient mice (Fig 2C, D). Intriguingly, inflammation did not further compromise the long-term repopulating ability of the DKO HSCs, compared to either single KO HSC, in both 16-week primary recipients and secondary transplanted recipients (Fig 2C, D). This inflammatory effect on the KO HSCs was confirmed by a limiting dilution assay, in which TNF- $\alpha$  treatment did not cause further reduction in the frequency of CRU in DKO HSCs as compared to either *FANCD2*-KO or *HES1*-KO HSCs (Fig 2E, Table III). Taken together, these results suggest that both *FANCD2* and *HES1* are required for limiting detrimental effects of inflammation on HSCs.

## Repression of inflammation-responsive $PPAR_{\gamma}$ expression requires both FANCD2 and HES1

Since HES1 suppresses inflammation-induced  $PPAR_{\gamma}$  expression,<sup>21,44-46</sup> and since several components of the FA pathway interact with HES1 and *HES1* deficiency causes a FA-like phenotype,<sup>41,42</sup> we examined the effect of *HES1* deficiency on  $PPAR_{\gamma}$  expression in inflammation-primed WT and *FANCD2*-KO HSCs. We found that TNF- $\alpha$  treatment induced an elevation of  $PPAR_{\gamma}$  expression with similar magnitude and kinetics in *FANCD2*-KO and *HES1*-KO SLAM cells compared to WT cells (Fig 3A). Significantly, deletion of *HES1* de-repressed  $PPAR_{\gamma}$  expression in WT but had no further effect on *FANCD2*-KO SLAM cells (Fig 3B). These results suggest that FANCD2 might co-operate with HES1 in  $PPAR_{\gamma}$  repression in HSCs. To test this idea, we measured the activity of  $PPAR_{\gamma}$  promoter, using a -1.5 kb  $PPAR_{\gamma}$  promoter-luciferase reporter,<sup>44</sup> in response to ectopic expression of FANCD2 and HES1. Primary mouse embryonic fibroblasts (MEFs) transfected with the  $PPAR_{\gamma}$ -luciferase reporter showed robust luciferase activity induced by TNF- $\alpha$  treatment (Fig 3C). Ectopic expression of HES1 had marginal effect in the absence of FANCD2 expression vector or *vice versa*; however, the repression of the reporter activity was enhanced synergistically when both FANCD2 and HES1 expression vectors were present (Fig 3C). These results indicate that FANCD2 is required for the repression of  $PPAR_{\gamma}$  promoter transcription by HES1.

To provide additional evidence for the ability of FANCD2 to enhance HES1 repressor activity on the  $PPAR_{\gamma}$  promoter, we performed a chromatin immunoprecipitation (ChIP) assay in BM Lin<sup>-</sup> cells from our recently generated *FANCD2*-KO mice, in which a dual tandem (3XFLAG and HA) tag was inserted at the C-terminus of the endogenous *FANCD2* locus.<sup>34</sup> We analyzed FANCD2 and HES1 occupancy along the 5-flanking region of the  $PPAR_{\gamma}$  gene extending from -1.5 kb to the transcriptional start site (Fig 3D). We detected strong inflammation-responsive binding of HES1 in the previously characterized B class E box (CANGTG, -771) and weaker binding at the N class E box (CACNAG, -535) in the *PPAR\_{\gamma}1* promoter (Fig 3D), consensus HES1-binding sites;<sup>45,47</sup> Significantly, FANCD2 was also found to occupy these  $PPAR_{\gamma}$  B/N E box elements in an inflammation-responsive manner (Fig 3E). These results provide biochemical evidence that FANCD2 is co-localized with HES1 on the regulatory region of the  $PPAR_{\gamma}$  gene.

## Gene-expression profiling reveals an overlapping deregulated FAO/OXPHOS/cell-cycle transcriptional programme in HSPCs deficient for FANCD2 and HES1

To address the downstream biology of the coordinate action by FANCD2 and HES1 in  $PPAR_{\gamma}$  repression, we performed gene-expression profiling by RNA-sequencing (RNA-seq) analysis to compare the FANCD2 and HES1 transcriptomes in LSK cells. We found that the inflammation-responsive transcriptional programmes engaged by FANCD2 and HES1 deficiencies were highly overlapping, with approximately 30% of deregulated genes induced by *FANCD2* deletion overlapping with those induced by *HES1* deletion (Fig 4A). We then conducted pathway analysis to identify the deregulated pathways that are shared by *FANCD2* and *HES1* deficiency. We identified three overlapping pathways: fatty acid oxidation (FAO), oxidative phosphorylation (OXPHOS) and cell-cycle control (Fig 4A, B). We validated the RNA-seq results for selected genes in these three pathways (Fig 4C). These

data indicate that inflammation orchestrates an overlapping transcriptional programme in HSPCs deficient for *FANCD2* and *HES1*.

### Augmented FAO in HSPCs deficient for *FANCD2* and *HES1*

The coordinative *PPAR<sub>γ</sub>* repression by *FANCD2* and *HES1* and the overlapping transcriptional regulation in the FAO pathway in *FANCD2*- and *HES1*-deficient HSPCs suggest that *FANCD2* and *HES1* may regulate this metabolic pathway in HSPCs. To test his notion, we first measured mitochondrial FAO in WT, *FANCD2*-KO, *HES1*-KO and DKO LSK cells treated with or without TNF- $\alpha$ . We found that loss of *FANCD2* or *HES1* augmented both basal and inflammation-primed FAO, as determined by the palmitate oxidation method (Fig 5A). However, concomitant loss of *FANCD2* and *HES1* did not further augment either basal or inflammation-primed FAO Fig 5A. To assess whether the augmented FAO was the consequence of *PPAR<sub>γ</sub>* de-repression, we treated WT, *FANCD2*-KO, *HES1*-KO or DKO LSK cells with a *PPAR<sub>γ</sub>* antagonist (GW9662)<sup>32</sup> and found that 5  $\mu$ M of GW9662 effectively reduced the inflammation-primed FAO in *FANCD2*-KO, *HES1*-KO and DKO LSK cells Fig 5B. To substantiate these findings, we performed shRNA knockdown of *CPT1*, which encodes the mitochondrial carnitine palmitoyltransferase-1, a rate-limiting enzyme in mitochondrial FAO.<sup>48</sup> We obtained one *CPT1* SFLV-eGFP-shCpt1 (shRNA) (*CPT1* #1) that showed efficient knockdown Fig S3. Using this *CPT1* shRNA, we were able to show that knockdown of *CPT1* almost completely reduced the inflammation-primed FAO in *FANCD2*-KO, *HES1*-KO and DKO LSK cells Fig 5C.

We then asked whether inhibition of the inflammation-primed FAO could improve function of the KO HSCs. To this end, we isolated LSK cells from WT, *FANCD2*-KO, *HES1*-KO or DKO mice, treated the inflammation-primed cells with the *PPAR<sub>γ</sub>* antagonist GW9662 or the mitochondrial FAO inhibitor etomoxir,<sup>49</sup> and transplanted the cells into lethally irradiated BoyJ recipients. We found that inhibition of *PPAR<sub>γ</sub>* by GW9662 partially rescued the inflammation-induced long-term repopulation defects of *FANCD2*-KO, *HES1*-KO or DKO HSCs in the transplanted recipients 16 weeks post BMT (Fig 5D). Similar improvement was also observed with the effect of the mitochondrial FAO inhibitor Etomoxir Fig 5D. Furthermore, inhibition of *PPAR<sub>γ</sub>* by GW9662 or of FAO by etomoxir significantly increased the frequency of CRUs in the limiting dilution assay (Fig 5E and Table IV). These results indicate that inhibition of inflammation-primed FAO improves the function of HSCs deficient for *FANCD2* and *HES1*.

### Genetic inhibition of *PPAR<sub>γ</sub>* or *CPT1* restores quiescence in HSCs deficient for *FANCD2* and *HES1*

Since we observed an overlapping upregulation of genes involved in the cell-cycle pathway in *FANCD2*-KO and *HES1*-KO HSPCs (Fig 4), we wondered whether the inflammation-induced exhaustion of *FANCD2*-KO and *HES1*-KO HSCs was due to loss of stem cell quiescence. We first determined the effect of *PPAR<sub>γ</sub>* knockdown on quiescence of *FANCD2*-KO and *HES1*-KO HSCs. We transduced WT, *FANCD2*-KO, *HES1*-KO or DKO HSCs with lentiviral vector expressing scramble shRNA or shRNA targeting *PPAR<sub>γ</sub>* and observed efficient knocking down of *PPAR<sub>γ</sub>* (Fig 6A, Figure S4). We found that depletion of *PPAR<sub>γ</sub>* significantly reduced inflammation-primed FAO (Fig 6B) and restored quiescence of

*FANCD2*-KO, *HES1*-KO and DKO HSCs (Fig 6C), as determined by palmitate oxidation assay and Ki67/DAPI staining, respectively. Similar results were found in *FANCD2*-KO, *HES1*-KO and DKO HSCs expressing shRNA targeting *CPT1* Fig 6D, in which *CPT1* knockdown significantly reduced inflammation-primed FAO (Fig 6E) and improved quiescence in *FANCD2*-KO, *HES1*-KO and DKO HSCs (Fig 6F). Taken together, these data suggest that targeted inhibition of *PPAR $\gamma$*  or *CPT1* restores quiescence in *FANCD2*-KO and *HES1*-KO HSCs.

## Discussion

Haematopoietic stem cell failure is now considered the root cause of FA BMF and leukaemia. However, the mechanisms by which FA proteins function in HSC maintenance remain largely unknown. In this work, we have identified a novel role of *FANCD2*, a key factor of the FA pathway, in regulating *HES1*-mediated transcriptional repression of *PPAR $\gamma$*  in HSC maintenance. We have provided several lines of evidence to support the notion: (i) deletion of *HES1* exacerbates *FANCD2*-KO HSC defects in steady state; (ii) both *FANCD2* and *HES1* are required for limiting the detrimental effects of inflammation on HSCs; (iii) repression of inflammation-induced transcription of the *PPAR $\gamma$*  gene requires both *FANCD2* and *HES1*; (iv) inflammation orchestrates an overlapping transcriptional programme in HSPCs deficient for *FANCD2* and *HES1*; (v) loss of *FANCD2* or *HES1* augments FAO in HSPCs, but concomitant loss of *FANCD2* and *HES1* did not further augment either basal or inflammation-primed FAO; and (vi) targeted inhibition of *PPAR $\gamma$*  or *CPT1* reduces FAO and restores quiescence in *FANCD2*-KO and *HES1*-KO HSCs.

The current study is the first demonstrating an *in vivo* functional interaction between the FA and *HES1*/Notch pathways. *HES1* is a member of the hairy-related basic helix–loop–helix (bHLH) family,<sup>18</sup> and an evolutionarily conserved target of Notch signaling, which regulates several cellular processes, including cell fate decisions and proliferation in both invertebrates and mice.<sup>50,51</sup> The crosstalk between the FA and the *HES1*/Notch pathways has been highlighted in recent reports showing that *HES1* interacts with several members of the FA core complex, including *FANCA*, *FANCF*, *FANCG* and *FANCL*.<sup>41,42</sup> Cells depleted of *HES1* exhibit an FA-like phenotype that includes cellular hypersensitivity to interstrand crosslinker mitomycin C (MMC), and lack of *FANCD2* monoubiquitination and foci formation.<sup>42</sup> *HES1* is also required for proper nuclear localization or stability of some members of the FA core complex.<sup>42</sup> We recently showed that inflammation-mediated deregulation of Notch signaling skewed HSC differentiation in FA mice. Specifically, we found that inflammation-enhanced Notch signalling leads to increased production of multipotential progenitors (MPPs) in FA mice.<sup>6</sup> The current study employed the *FANCD2*-KO and *HES1*-KO mouse models to show that both *FANCD2* and *HES1* are required for limiting the detrimental effects of inflammation on HSCs and that repression of inflammation-induced *PPAR $\gamma$*  expression requires both *FANCD2* and *HES1*. Furthermore, inflammation orchestrated an overlapping transcriptional programme in HSPCs deficient for *FANCD2* and *HES1*, featuring upregulated genes in the FAO metabolic pathway. Consistently, we observed that deletion of *FANCD2* or *HES1* in mouse HSCs resulted in a marked increase in FAO and that targeted inhibition of FAO improved the *in vivo* function of

these mutant HSCs. These findings add another layer to the current understanding of the role of FA proteins in HSC maintenance.

It is intriguing that while concomitant deletion of *HES1* exacerbates *FANCD2*-KO HSC defects in the steady state, inflammation does not further decrease self-renewal of DKO HSCs. In addition, inflammation does not further compromise long-term repopulating ability of the DKO HSCs. The observation that DKO mice exhibit more severe HSC defects than either *HES1*-KO or *FANCD2*-KO cells suggests that multiple (Notch and FA) pathway deficiencies additively affect the function of DKO HSCs. In response to inflammatory cues, however, both *FANCD2* and *HES1* are required for limiting detrimental effects of inflammation on HSCs. This is accomplished by a co-ordinative action of *FANCD2* and *HES1* to negatively regulate *PPAR $\gamma$*  expression and consequently mitochondrial FAO, as loss of either *FANCD2* or *HES1* leads to the same magnitude of increase in *PPAR $\gamma$*  expression and FAO in HSCs. This functional outcome would indicate the interaction between *FANCD2* and *HES1*/*PPAR $\gamma$* /FAO pathways plays a major role in HSC function under inflammatory stress.

It has been shown that several components of the FA core complex interact with *HES1* and *HES1* deficiency causes a FA-like phenotype.<sup>41,42</sup> Our current study suggests that repression of inflammation-activated *PPAR $\gamma$*  transcription by *HES1* may require not only *FANCD2* but also the upstream FA core complex. Specifically, we propose that the formation of the *FANCD2*-*HES1* co-repressor complex may require the FA core complex or *FANCD2* mono-ubiquitination. Previous studies have shown that mice deficient for several components of the FA core complex (e.g. *FANCA*, *FANCB*, *FANCC*, *FANCG*) exhibit extremely similar HSC defect phenotypes as those deleted for *FANCD2*.<sup>13,40</sup> We therefore further propose that HSCs deficient for the FA core or defective in *FANCD2* mono-ubiquitination<sup>17</sup> would fail to form a functional *FANCD2*-*HES1* co-repressor complex, and consequently lead to de-repressed *PPAR $\gamma$*  transcription and FAO induced by inflammation. Thus, further investigation on this novel *FANCD2*/*HES1*/*PPAR $\gamma$*  signalling axis will provide critical insights into the regulatory role of the FA pathway in inflammation-responsive *PPAR $\gamma$*  expression and FAO during HSC maintenance.

Mechanistically, our results show that *FANCD2* and *HES1* acted in concert to repress the *PPAR $\gamma$*  promoter in an inflammation-responsive manner and that loss of *FANCD2* or *HES1* led to de-repression of inflammation-induced *PPAR $\gamma$*  expression and augmented FAO. Although attempts to identify a biochemical *FANCD2*-*HES1* complex were unsuccessful (data not shown), we envision that *FANCD2* and *HES1* form a functional co-repressor complex in the context of inflammation-responsive *PPAR $\gamma$*  expression, and the relevance of this transcriptional complex to the deregulated mitochondrial FAO is critical for understanding the novel role of the *FANCD2*/FA pathway in immunometabolic regulation. In addition, *FANCD2* and *HES1* co-occupied the B/N E box elements (consensus *HES1*-binding sites) of the *PPAR $\gamma$*  promoter in an inflammation-responsive manner. Functionally, we show that the increased mitochondrial FAO, induced by inflammation-responsive *PPAR $\gamma$*  expression, promotes HSC cycling and consequently HSC exhaustion. These findings argue that dysregulated *PPAR $\gamma$* /FAO also compromises the regenerative capacity of HSCs and constitutes a contributing factor for HSC defect. We recently found that FA HSCs are more



dependent on mitochondrial respiration relative to glycolysis in their resting state for energy metabolism.<sup>37,52</sup> More recently, by employing an *in vivo* RNAi screen (The shRNA library pool was provided by Dr. Lenhard Rudolph (Max-Planck-Research Institute) using SFFV EcoR1-Egfp-shRNA vector), we identified PPAR<sub>γ</sub>, a central transcription factor regulating adipocyte differentiation and energy metabolism, as a regulator of HSC homeostasis.<sup>31</sup> It has also been shown that inhibition of PPAR<sub>γ</sub> improves *ex vivo* expansion of human HSCs and progenitors by enhancing glycolysis.<sup>32</sup> Nevertheless, how HES1 regulates PPAR<sub>γ</sub> signaling and the FAO metabolic pathway in HSCs is less understood. We recently identified a novel role for HES1 in regulating haematopoiesis under stress condition through regulating PPAR<sub>γ</sub> signalling pathway and fatty acid metabolism pathways using a haematopoietic lineage-specific *HES1* knockout mouse model (*HES1<sup>fl/fl</sup>Vav1Cre*).<sup>25</sup> Combined with our current study showing that FANCD2 and HES1 are required to repress PPAR<sub>γ</sub> expression and mitochondrial FAO in response to inflammatory stress, we propose that the novel FANCD2/HES1/PPAR<sub>γ</sub> may constitute a key component of immunometabolic regulation, connecting inflammation, cellular metabolism and HSC function.

## Supplementary Material

Refer to Web version on PubMed Central for supplementary material.

## Acknowledgements

We thank Dr. Markus Grompe (Oregon Health & Sciences University) for *FANCD2<sup>+/-</sup>* mice, Dr. Ryoichiro Kageyama (Kyoto University) for *HES1<sup>fl/fl</sup>* mice. This work is supported by a NIH/NHLBI grant (R01HL151390 to WD).

## Data availability statement

The data that support the findings of this study are available from their corresponding author upon reasonable request.

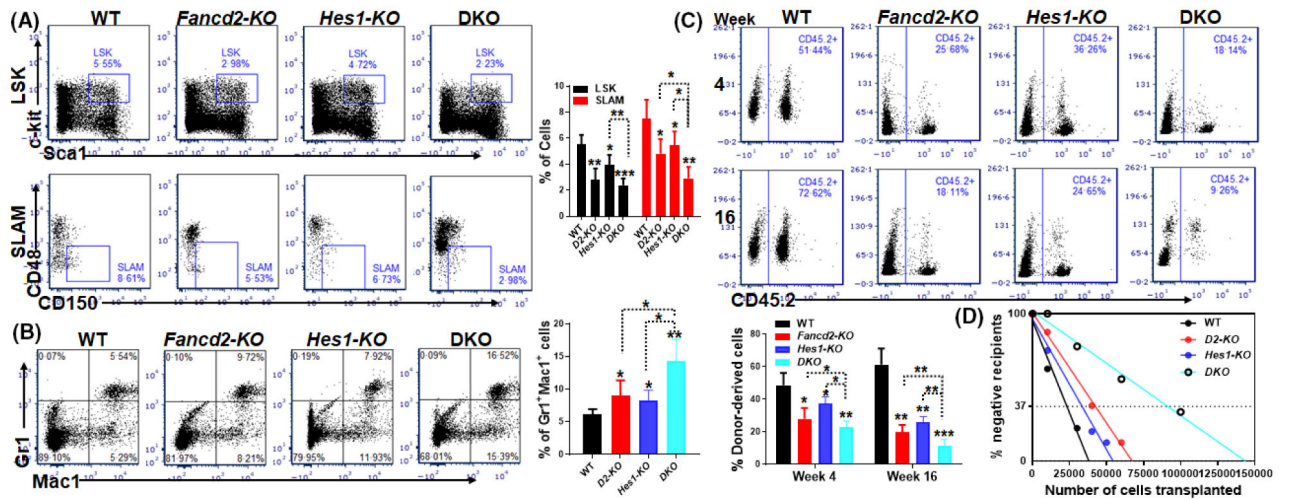
## References

1. Bagby GC, Alter BP. Fanconi anemia. *Semin Hematol.* 2006;43(3):147–56. [PubMed: 16822457]
2. Schneider M, Chandler K, Tischkowitz M, Meyer S, Fanconi anaemia: genetics, molecular biology, and cancer – implications for clinical management in children and adults. *Clin Genet.* 2015;88(1):13–24. [PubMed: 25307146]
3. Deans AJ, West SC. DNA interstrand crosslink repair and cancer. *Nat Rev Cancer.* 2011;11:467–80. [PubMed: 21701511]
4. Kim H, D'Andrea AD. Regulation of DNA cross-link repair by the Fanconi anemia/BRCA pathway. *Genes Dev.* 2012;26:1393–408. [PubMed: 22751496]
5. Haneline LS, Li X, Ciccone SL, Hong P, Yang Y, Broxmeyer HE, et al. Retroviral-mediated expression of recombinant Fancc enhances the repopulating ability of *Fancc<sup>-/-</sup>* hematopoietic stem cells and decreases the risk of clonal evolution. *Blood.* 2003;101(4):1299–307. [PubMed: 12393504]
6. Kelly PF, Radtke S, von Kalle C, Balcik B, Bohn K, Mueller R, et al. Stem cell collection and gene transfer in Fanconi anemia. *Mol Ther.* 2007;15(1):211–9. [PubMed: 17164793]
7. Du W, Amarachintha S, Sipple J, Schick J, Pang Q. Inflammation-mediated Notch signaling skews Fanconi Anemia hematopoietic stem cell differentiation. *J Immunol.* 2013;191(5):2806–17. [PubMed: 23926327]

8. Du W, Amarachintha S, Erden O, Wilson A, Meetei AR, Andreassen PR, et al. Fancb deficiency impairs hematopoietic stem cell function. *Sci Rep.* 2015;5:18127. [PubMed: 26658157]
9. Haneline LS, Gobbett TA, Ramani R, Carreau M, Buchwald M, Yoder MC, et al. Loss of FancC function results in decreased hematopoietic stem cell repopulating ability. *Blood.* 1999;94(1):1–8. [PubMed: 10381491]
10. Li X, Li J, Wilson A, Sipple J, Schick J, Pang Q. Fancd2 is required for nuclear retention of Foxo3a in hematopoietic stem cell maintenance. *J Biol Chem.* 2015;290(5):2715–27. [PubMed: 25505262]
11. Li X, Wilson AF, Du W, Pang Q. Cell-Cycle-Specific Function of p53 in Fanconi Anemia Hematopoietic Stem and Progenitor Cell Proliferation. *Stem Cell Reports.* 2018;10(2):339–46. [PubMed: 29307578]
12. Li J, Sejas DP, Zhang X, Qiu Y, Nattamai KJ, Rani R, et al. TNF- $\alpha$  induces leukemic clonal evolution *ex vivo* in Fanconi anemia group C stem cells. *J Clin Invest.* 2007;117:3283–95. [PubMed: 17960249]
13. Lensch MW, Rathbun RK, Olson SB, Jones GR, Bagby GC Jr. Selective pressure as an essential force in molecular evolution of myeloid leukemic clones: a view from the window of Fanconi anemia. *Leukemia.* 1999;13:1784–9. [PubMed: 10557053]
14. Auerbach AD, Allen RG. Leukemia and preleukemia in Fanconi anemia patients. A review of the literature and report of the International Fanconi Anemia Registry. *Cancer Genet Cytogenet.* 1991;51:1–12. [PubMed: 1984836]
15. Kutler DI, Singh B, Satagopan J, Batish SD, Berwick M, Giampietro PF, et al. A 20-year perspective on the International Fanconi Anemia Registry (IFAR). *Blood.* 2003;101:1249–56. [PubMed: 12393516]
16. Kalb R, Neveling K, Hoehn H, Schneider H, Linka Y, Batish SD, et al. Hypomorphic mutations in the gene encoding a key Fanconi anemia protein, FANCD2, sustain a significant group of FA-D2 patients with severe phenotype. *Am J Hum Genet.* 2007;80:895–910. [PubMed: 17436244]
17. Parmar K, Kim J, Sykes SM, Shimamura A, Stuckert P, Zhu K, et al. Hematopoietic stem cell defects in mice with deficiency of Fancd2 or Usp1. *Stem Cells.* 2010;28:1186–95. [PubMed: 20506303]
18. Kageyama R, Ohtsuka T, Kobayashi T. The Hes gene family: repressors and oscillators that orchestrate embryogenesis. *Development.* 2007;134:1243–51. [PubMed: 17329370]
19. Kawamata S, Du C, Li K, Lavau C. Overexpression of the Notch target genes Hes in vivo induces lymphoid and myeloid alterations. *Oncogene.* 2002;21:3855–63. [PubMed: 12032823]
20. Tomita K, Hattori M, Nakamura E, Nakanishi S, Minato N, Kageyama R. The bHLH gene Hes1 is essential for expansion of early T cell precursors. *Genes Dev.* 1999;13:1203–10. [PubMed: 10323870]
21. Espinosa L, Cathelin S, D'Altri T, et al. The Notch/Hes1 pathway sustains NF- $\kappa$ B activation through CYLD repression in T cell leukemia. *Cancer Cell.* 2010;18(3):268–81. [PubMed: 20832754]
22. Wendorff AA, Koch U, Wunderlich FT, Wirth S, Dubey C, Brüning JC, et al. Hes1 is a critical but context-dependent mediator of canonical Notch signaling in lymphocyte development and transformation. *Immunity.* 2010;33:671–84. [PubMed: 21093323]
23. Kunisato A, Chiba S, Nakagami-Yamaguchi E, Kumano K, Saito T, Masuda S, et al. HES-1 preserves purified hematopoietic stem cells *ex vivo* and accumulates side population cells *in vivo*. *Blood.* 2003;101:1777–83. [PubMed: 12406868]
24. Varnum-Finney B, Xu L, Brashem-Stein C, Nourigat C, Flowers D, Bakkour S, et al. Pluripotent, cytokine-dependent, hematopoietic stem cells are immortalized by constitutive Notch1 signaling. *Nat Med.* 2000;6:1278–81. [PubMed: 11062542]
25. Ma Z, Xu J, Wu L, Wang JJ, Lin Q, Chowdhury FA, et al. Hes1 deficiency causes hematopoietic stem cell exhaustion. *Stem Cells.* 2020;38(6):756–68. [PubMed: 32129527]
26. Karigane D, Takubo K. Metabolic regulation of hematopoietic and leukemic stem/progenitor cells under homeostatic and stress conditions. *Int J Hematol.* 2017;106(1):18–26. [PubMed: 28540498]
27. Suda T, Takubo K, Semenza GL. Metabolic regulation of hematopoietic stem cells in the hypoxic niche. *Cell Stem Cell.* 2011;9:298–310. [PubMed: 21982230]

28. Warr MR, Pietras EM, Passequé E. Mechanisms controlling hematopoietic stem cell functions during normal hematopoiesis and hematological malignancies. *Rev Syst Biol Med*. 2011;3(6):681–701.
29. Baumann K Stem cells: A metabolic switch. *Nat Rev Mol Cell Biol*. 2013;14(2):64–5.
30. Kersten S, Desvergne B, Wahli W. Roles of PPARs in health and disease. *Nature*. 2000;405(6785):421–4. [PubMed: 10839530]
31. Sertorio M, Du W, Amarachintha S, Wilson A, Pang Q. In Vivo RNAi screen unveils PPAR $\gamma$  as a regulator of hematopoietic stem cell homeostasis. *Stem Cell Reports*. 2017;8(5):1242–55. [PubMed: 28416286]
32. Guo B, Huang X, Lee MR, Lee SA, Broxmeyer HE. Antagonism of PPAR- $\gamma$  signaling expands human hematopoietic stem and progenitor cells by enhancing glycolysis. *Nat Med*. 2018;24(3):360–7. [PubMed: 29377004]
33. Houghtaling S, Timmers C, Noll M, Finegold MJ, Jones SN, Meyn MS, et al. Epithelial cancer in Fanconi anemia complementation group D2 (Fancd2) knockout mice. *Genes Dev*. 2003;17(16):2021–35. [PubMed: 12893777]
34. Imayoshi I, Shimogori T, Ohtsuka T, Kageyama R. Hes genes and neurogenin regulate non-neural versus neural fate specification in the dorsal telencephalic midline. *Development*. 2008;135(15):2531–41. [PubMed: 18579678]
35. Zhang T, Du W, Wilson AF, Namekawa SH, Andreassen PR, Meetei AR, et al. Fancd2 in vivo interaction network reveals a non-canonical role in mitochondrial function. *Sci Rep*. 2017;7:45626. [PubMed: 28378742]
36. Kiel MJ, Yilmaz OH, Iwashita T, Yilmaz OH, Terhorst C, Morrison SJ. SLAM family receptors distinguish hematopoietic stem and progenitor cells and reveal endothelial niches for stem cells. *Cell*. 2005;121:1109–21. [PubMed: 15989959]
37. Du W, Amarachintha S, Wilson AF, Pang Q. SCO2 mediates oxidative stress-induced glycolysis to OXPHOS switch in hematopoietic stem cells. *Stem Cells*. 2016;34(4):960–71. [PubMed: 26676373]
38. Liu ZG. Molecular mechanism of TNF signaling and beyond. *Cell Res*. 2005;15(1):24–7. [PubMed: 15686622]
39. Bazzoni F, Beutler B. The tumor necrosis factor ligand and receptor families. *N Engl J Med*. 1996;334(26):1717–25. [PubMed: 8637518]
40. Du W, Erden O, Pang Q. TNF- $\alpha$  signaling in Fanconi anemia. *Blood Cells Mol. Dis*. 2014;52(1):2–11. [PubMed: 23890415]
41. Tremblay CS, Huang FF, Habi O, Huard CC, Godin C, Lévesque G, et al. HES1 is a novel interactor of the Fanconi anemia core complex. *Blood*. 2008;112(5):2062–70. [PubMed: 18550849]
42. Tremblay CS, Huard CC, Huang FF, Habi O, Bourdages V, Lévesque V, et al. The fanconi anemia core complex acts as a transcriptional co-regulator in hairy enhancer of split 1 signaling. *J Biol Chem*. 2009;284 (20):13384–95. [PubMed: 19321451]
43. Dufour C, Corcione A, Svahn J, Haupt R, Poggi V, Béka'ssy AN, et al. TNF-alpha and IFN-gamma are overexpressed in the bone marrow of Fanconi anemia patients and TNF-alpha suppresses erythropoiesis in vitro. *Blood*. 2003;102(6):2053–9. [PubMed: 12750172]
44. Maniati E, Bossard M, Cook N, Candido JB, Emami-Shahri N, Nedospasov SA, et al. Crosstalk between the canonical NF- $\kappa$ B and Notch signaling pathways inhibits Ppar $\gamma$  expression and promotes pancreatic cancer progression in mice. *J Clin Invest*. 2011;121(12):4685–99. [PubMed: 22056382]
45. Herzig S, Hedrick S, Morantte I, Koo SH, Galimi F, Montminy M. CREB controls hepatic lipid metabolism through nuclear hormone receptor PPAR-gamma. *Nature*, 426(6963), 190–3. [PubMed: 14614508]
46. Renström J, Istvanffy R, Gauthier K, Shimono A, Mages J, Jardon-Alvarez A, et al. Secreted frizzled-related protein 1 extrinsically regulates cycling activity and maintenance of hematopoietic stem cells. *Cell Stem Cell*. 2009;5(2):157–67. [PubMed: 19664990]
47. Iso T, Kedes L, Hamamori Y. HES and HERP families: multiple effectors of the Notch signaling pathway. *J Cell Physiol*. 2003;194(3):237–55. [PubMed: 12548545]

48. Briant LJB, Dodd MS, Chibalina MV, Rorsman NJG, Johnson PRV, Carmeliet P, et al. CPT1a-dependent long-chain fatty acid oxidation contributes to maintaining glucagon secretion from pancreatic islets. *Cell Rep.* 2018;23(11):3300–11. [PubMed: 29898400]
49. Vats D, Mukundan L, Odegaard JI, Zhang L, Smith KL, Morel CR, et al. Oxidative metabolism and PGC-1 $\beta$  attenuate macrophage-mediated inflammation. *Cell Metab.* 2006;4:13–24. [PubMed: 16814729]
50. Jarriault S, Brou C, Logeat F, Schroeter EH, Kopan R, Israel A. Signalling downstream of activated mammalian notch. *Nature.* 1995;377:355–8. [PubMed: 7566092]
51. Nishimura M, Isaka F, Ishibashi M, Tomita K, Tsuda H, Nakanishi S, et al. Structure, chromosomal locus, and promoter of mouse Hes2 gene, a homologue of *Drosophila* hairy and enhancer of split. *Genomics.* 1998;49:69–75. [PubMed: 9570950]
52. Li X, Wu L, Zopp M, Kopelov S, Du W. p53-TIGAR axis-mediated glycolytic suppression attenuates DNA damage and genomic instability in Fanconi anemia hematopoietic stem cells. *Stem Cells.* 2019;37(7):937–47. [PubMed: 30977208]

**Fig 1.**

Loss of *HES1* exacerbates *FANCD2*-KO HSC defects. (A) Loss of *HES1* further decreases the haematopoietic stem and progenitor cell (HSPC) pool in *FANCD2*-KO mice. Whole bone marrow cells (WBMCs) isolated from 8–10-weeks-old WT, *FANCD2*-KO, *HES1*-KO or *FANCD2*;*HES1* double knockout (DKO) mice were subjected to flow cytometry analysis for LSK (Lin<sup>-</sup>Sca1<sup>+</sup>c-kit<sup>+</sup>) and signaling lymphocyte activation molecule (SLAM; LSKCD150<sup>+</sup>CD48<sup>-</sup>) populations. Representative flow plots (left) and quantification (right) are shown. Results are means  $\pm$  standard deviation (*SD*) of three independent experiments ( $n = 9$  per group). (B) *HES1* deficiency leads to more severe myeloid skew in *FANCD2*-KO mice. Cells described in (A) were subjected to flow cytometry analysis for myeloid lineages (Gr1 and Mac1). Representative flow plots (left) and quantification (right) are shown. Results are means  $\pm$  *SD* of three independent experiments ( $n = 9$  per group). (C) Loss of *HES1* further compromises repopulating defects of *FANCD2*-KO cells. One million WBMCs isolated from WT, *FANCD2*-KO, *HES1*-KO or DKO mice (CD45.2<sup>+</sup>), along with equal numbers of congenic WBMCs from BoyJ mice (CD45.1<sup>+</sup>), were transplanted into lethally irradiated BoyJ recipients. Donor-derived chimaera was detected by flow cytometry at four weeks and 16 weeks post bone marrow transplantation (BMT). Representative flow plots (upper) and quantification (lower) are shown. Results are means  $\pm$  *SD* of three independent experiments ( $n = 10$ –12 per group). (D) *HES1* deficiency leads to more severe HSC exhaustion in *FANCD2*-KO HSCs. Graded numbers of low-density bone marrow (BM) cells (LDBMCs) from WT, *FANCD2*-KO, *HES1*-KO or DKO mice, along with  $2 \times 10^5$  radio-protector BM cells from BoyJ mice (CD45.1<sup>+</sup>), were transplanted into lethally irradiated recipients. Plotted are the percentages of recipients containing less than 1% donor (CD45.2<sup>+</sup>) blood nucleated cells at 16 weeks post-transplantation. The frequency of functional HSCs was calculated according to Poisson statistic stem cells harbouring the capacities. Comparisons are WT *versus* single KO, and single KO vs DKO. \* $P < 0.05$ ; \*\* $P < 0.01$ ; \*\*\* $P < 0.001$ .

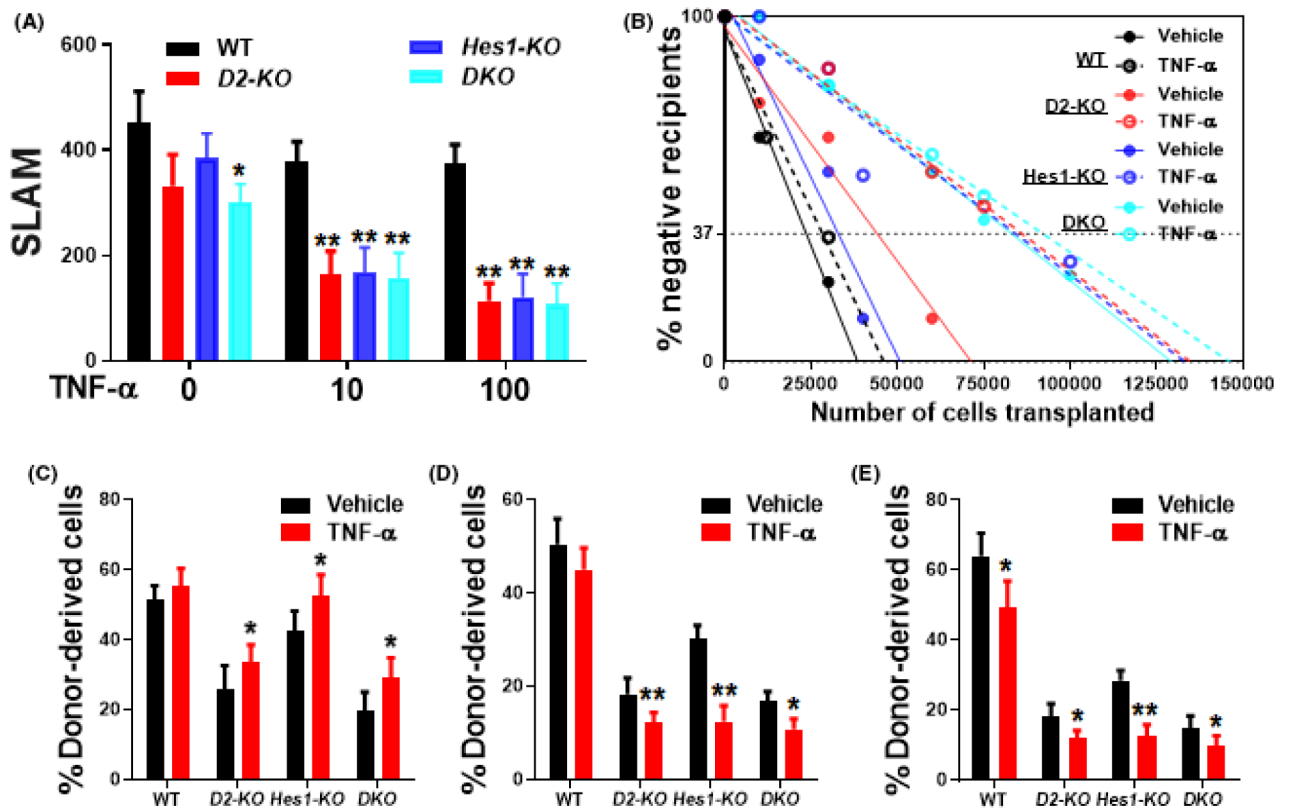


**Fig 2.**

Both *FANCD2* and *HES1* are required for limiting detrimental effects of inflammation on haematopoietic stem cells (HSCs). (A) Inflammation does not further decrease self-renewal capacity of double knockout (*DKO*) HSCs. One hundred signaling lymphocyte activation molecule (SLAM) cells isolated from WT, *FANCD2-KO*, *HES1-KO* or double knockout (*DKO*) mice were cultured in HSC medium in the presence or absence of indicated doses of TNF- $\alpha$ . The numbers of SLAM cells were determined by flow cytometry 10 days after culture. Results are means  $\pm$  standard deviation (SD) of three independent experiments. Comparisons are WT vs single KO or *DKO* for each indicated dosage. (B) Inflammation increases short-term repopulation. Five hundred SLAM cells ( $CD45.2^+$ ) pretreated with TNF- $\alpha$  (10 ng/ml) for 16 h, along with  $2 \times 10^5$  radio-protector BM cells from BoyJ mice ( $CD45.1^+$ ), were transplanted into lethally irradiated BoyJ recipients. Donor-derived chimaeras were detected at four weeks post bone marrow transplantation (BMT;  $n = 8-10$  per group). Comparisons are vehicle versus TNF- $\alpha$ . (C) Inflammation reduces long-term repopulation. Donor-derived chimaeras were detected at 16 week post BMT in the recipients described in (B) by flow cytometry ( $n = 8-10$  per group). Comparisons are vehicle versus TNF- $\alpha$ . (D) Inflammation does not further compromise long-term repopulating ability of *DKO* HSCs in secondary transplanted recipients. Three million whole bone marrow cells (WBMCs) from the primary recipients described in (B) were transplanted into sublethally irradiated BoyJ recipients. Donor-derived chimaeras were detected at 16 week post BMT ( $n = 10-12$  per group). Comparisons are vehicle versus TNF- $\alpha$ . (E) Inflammation does not cause more severe HSC exhaustion in *DKO* HSCs. Graded numbers of WBMCs isolated from WT, *FANCD2-KO*, *HES1-KO* or *DKO* mice ( $CD45.2^+$ ) were treated with TNF- $\alpha$  (10

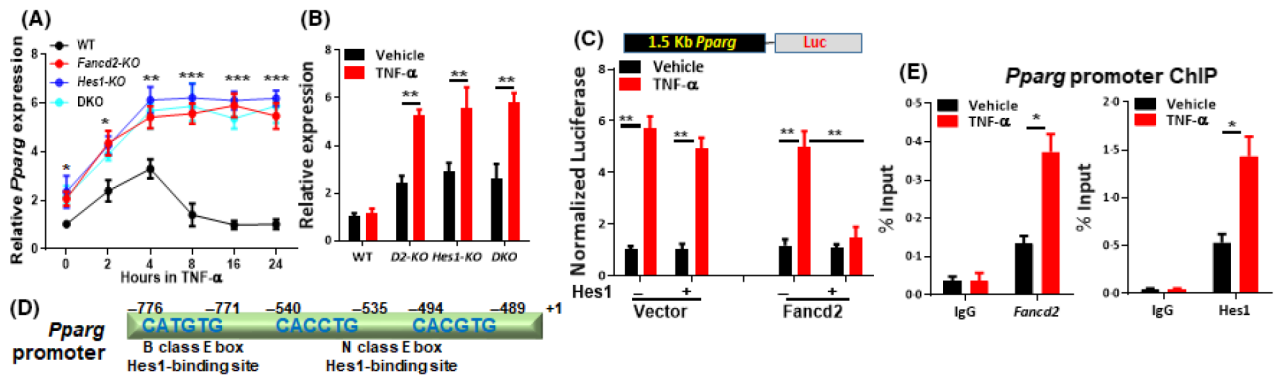
ng/ml) for 16 h, were transplanted along with  $2 \times 10^5$  radio-protector BM cells from BoyJ mice (CD45 $\cdot$ 1 $^+$ ), into lethally irradiated recipients. Plotted are the percentages of recipients containing less than 1% donor (CD45 $\cdot$ 2 $^+$ ) blood nucleated cells at 16 weeks post-transplantation. The frequency of functional HSCs was calculated according to Poisson statistic stem cells harbouring the capacities. \*,  $P < 0.05$ ; \*\*,  $P < 0.01$ .

Author Manuscript

Author Manuscript

Author Manuscript

Author Manuscript

**Fig 3.**

Repression of inflammation-induced *PPAR $\gamma$*  expression requires both FANCD2 and HES1. (A) Loss of *FANCD2* or *HES1* fails to repress inflammation-induced *PPAR $\gamma$*  expression. Bone marrow (BM) signaling lymphocyte activation molecule (SLAM) cells isolated from WT, *FANCD2*-KO, *HES1*-KO or double knockout (DKO) mice were treated with TNF- $\alpha$  (10 ng/ml) for the indicated time points. Expression of *PPAR $\gamma$*  was determined by real-time polymerase chain reaction (PCR). Results are means  $\pm$  standard deviation (*SD*) of three independent experiments. Comparisons are WT *versus* single KO or DKO for each indicated dosage. (B) Deletion of *HES1* in *FANCD2*-KO haematopoietic stem cells (HSCs) does not further increase *PPAR $\gamma$*  expression. BM SLAM cells isolated from WT, *FANCD2*-KO, *HES1*-KO or DKO mice were treated with TNF- $\alpha$  (10 ng/ml) for 16 h, and the expression levels of *PPAR $\gamma$*  mRNA were determined by real-time PCR. Results are means  $\pm$  *SD* of three independent experiments. Comparisons are vehicle *versus* TNF- $\alpha$ . (C) FANCD2 co-represses *PPAR $\gamma$*  expression. Mouse embryonic fibroblast (MEF) cells expressing a *PPAR $\gamma$*  reporter construct containing 1.5 kB of the proximal *PPAR $\gamma$*  promoter were co-transfected with HES1 and FANCD2 expression vectors. Subsequently, 24 h after transfection, cells were treated with TNF- $\alpha$  (10 ng/ml) for 16 h and analyzed for luciferase activity. Results are means  $\pm$  *SD* of three independent experiments. Comparisons are vehicle *versus* TNF- $\alpha$ . (D) Sequences of the consensus HES1-binding sites in the *PPAR $\gamma$*  promoter. +1 indicates transcription start site. (E) Inflammation-responsive recruitment of FANCD2 and HES1 to the endogenous *PPAR $\gamma$*  promoter. BM Lin<sup>-</sup> cells isolated from *Fancd2*-KO mice were treated with TNF- $\alpha$  (10 ng/ml) for 16 h, and ChIP assays were carried out using anti-FLAG, HES1 and control IgG. The regions encompassing the HES1-binding sites in the previously characterized B class E box (CANGTG; -771) in the *PPAR $\gamma$*  promoter were amplified by real-time PCR. Results are means  $\pm$  *SD* of three independent experiments. Comparisons are vehicle *versus* TNF- $\alpha$ . \*, *P* < 0.05; \*\*, *P* < 0.01; \*\*\*, *P* < 0.001.



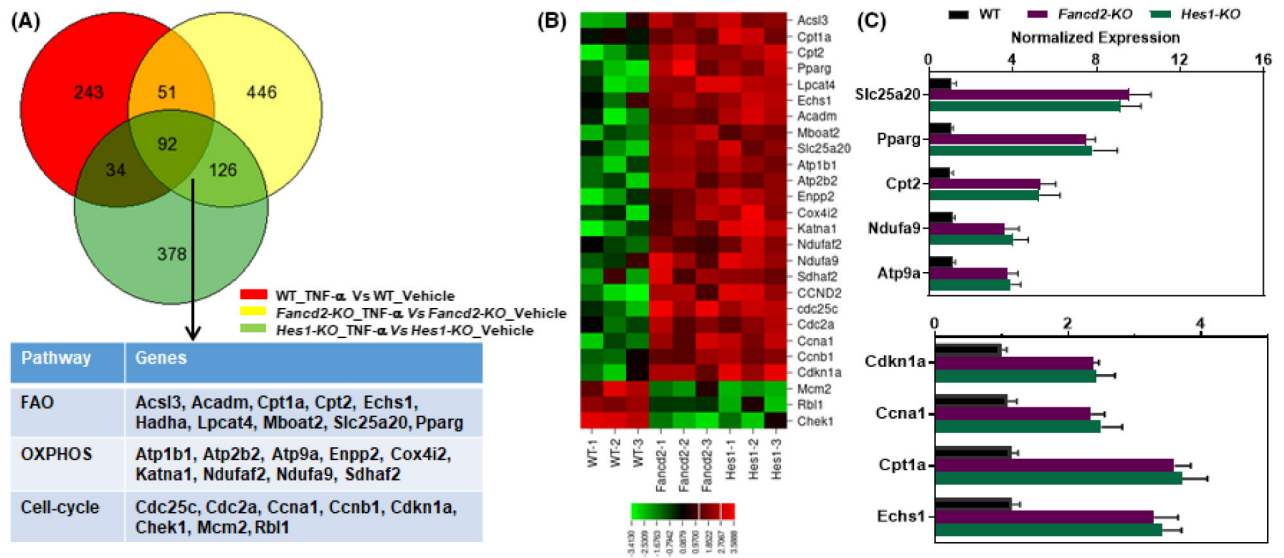


**Fig 4.** Overlapping deregulated fatty acid oxidation (FAO)/oxidative phosphorylation (OXPHOS)/cell-cycle transcriptional programme in *FANCD2*-KO and *HES1*-KO haematopoietic stem and progenitor cells (HSPCs). (A) Analysis of differential gene expression in WT, *FANCD2*-KO, *HES1*-KO Lin<sup>-</sup>Sca1<sup>+</sup>c-kit<sup>+</sup> (LSK) cells treated with TNF- $\alpha$  (10 ng/ml) for 16 h. Differentially expressed genes (0.05 *P* value cut-off, 2.0 fold change cut-off) in each group were used for pairwise comparison to identify unique and shared genes. Numbers depicted in the Venn diagram represent the up- and down-regulated genes in unique sections or shared genes in each intersection. Shared genes in *FANCD2*-KO and *HES1*-KO groups were further selected to run the pathway analysis module of GeneSpring GX v12 (Agilent, Santa Clara, CA, WikiPathway database (<https://www.wikipathways.org/index.php/WikiPathways>)) using the curated WikiPathway database. (B) Heatmap presentation of the genes in the three shared pathways. (C) Validation of gene expression changes from RNA-seq analysis by real-time polymerase chain reaction (PCR) Table S1. LSK cells from WT, *FANCD2*-KO, or *HES1*-KO mice were treated with TNF- $\alpha$  (10 ng/ml) for 16 h. Error bars represent mean  $\pm$  standard deviation (*SD*) of three independent experiments.

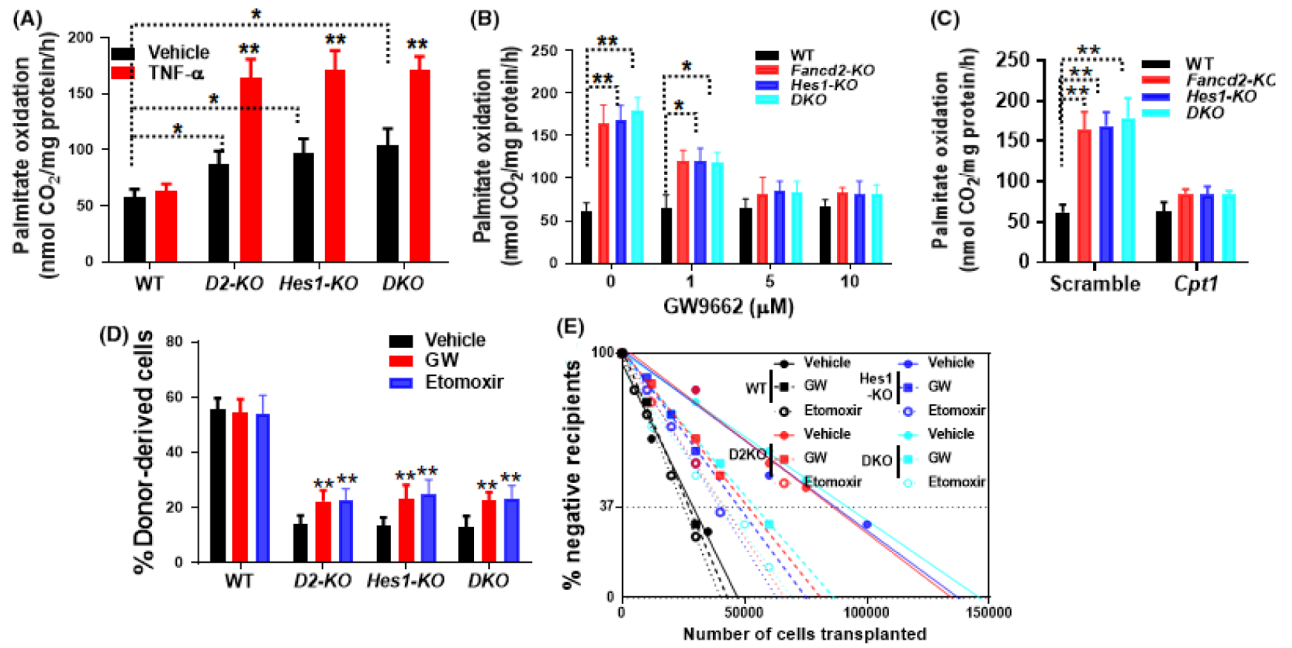


**Fig 5.**

Augmented fatty-acid oxidation (FAO) in haematopoietic stem and progenitor cells (HSPCs) deficient for *FANCD2* and *HES1* exhibit augmented FAO. (A) Loss of *FANCD2* or *HES1* augments both basal and inflammation-primed FAO. WT, *FANCD2*-KO, *HES1*-KO or double knockout (DKO) Lin<sup>-</sup>Sca1<sup>+</sup>c-kit<sup>+</sup> (LSK) cells were treated with TNF- $\alpha$  (10 ng/ml) for 16 h, and palmitate oxidation rates were assessed as captured <sup>14</sup>C<sub>2</sub> using the isolated mitochondria and 1-<sup>14</sup>C-palmitate as substrate. Results are means  $\pm$  standard deviation (SD) of three independent experiments. Comparisons are WT *versus* single or DKO; or vehicle *versus* TNF- $\alpha$ . (B) Pharmacological inhibition of PPAR $\gamma$  reduces FAO in *FANCD2*-KO, *HES1*-KO or DKO LSK haematopoietic stem and progenitor cells (HSPCs). Levels of inflammation-primed palmitate oxidation rates were measured in FAO in WT, *FANCD2*-KO, *HES1*-KO or DKO LSK cells treated with increasing concentrations of GW9662. Results are means  $\pm$  SD of three independent experiments. Comparisons are untreated *versus* treated groups. (C) Knockdown of *CPT1* reduces mitochondrial respiration. Levels of inflammation-primed palmitate oxidation rates were measured in WT, *FANCD2*-KO, *HES1*-KO or DKO LSK cells transduced with lentiviral vector expressing scramble shRNA or shRNA targeting *CPT1*. Results are means  $\pm$  SD of three independent experiments. Comparisons are WT *versus* single or DKO. (D) Pharmacological inhibition of PPAR $\gamma$  rescues long-term repopulation of DKO HSCs. LSK cells from WT, *FANCD2*-KO, *HES1*-KO or DKO mice were pretreated with TNF- $\alpha$  (10 ng/ml) for 2 h followed by treatment with GW9662 (5  $\mu$ M) or etomoxir (40  $\mu$ M) for an additional 14 h. Five thousand treated LSK cells (CD45<sup>+</sup>2<sup>+</sup>) along with  $2 \times 10^5$  radio-protector cells from congenic mice (CD45<sup>+</sup>1<sup>+</sup>) were transplanted into lethally irradiated BoyJ recipients. Donor-derived chimaeras were determined by flow cytometry 16 weeks post bone marrow transplantation (BMT;  $n = 10$ –12 per group). Comparisons are untreated *versus* treated groups. (E) Inhibition of mitochondrial respiration or suppression of PPAR $\gamma$  prevents HSC exhaustion in *FANCD2*-KO HSCs. Low-density bone marrow cells (LDBMCs) from WT, *FANCD2*-KO, *HES1*-KO or DKO mice

were pretreated with TNF- $\alpha$  followed by the treatment with vehicle, GW9662 or etomoxir as described in (D). Graded numbers of the treated cells (CD45 $\cdot$ 2 $^{+}$ ), along with  $2 \times 10^5$  radio-protector cells from congenic mice (CD45 $\cdot$ 1 $^{+}$ ), were then transplanted into lethally irradiated recipients. Plotted are the percentages of recipients containing less than 1% donor (CD45 $\cdot$ 2 $^{+}$ ) blood nucleated cells at 16 weeks post-transplantation. The frequency of functional HSCs was calculated according to Poisson statistic stem cells harbour the capacities. \*,  $P < 0.05$ ; \*\*,  $P < 0.01$ ; \*\*\*,  $P < 0.01$ .

Author Manuscript

Author Manuscript

Author Manuscript

Author Manuscript

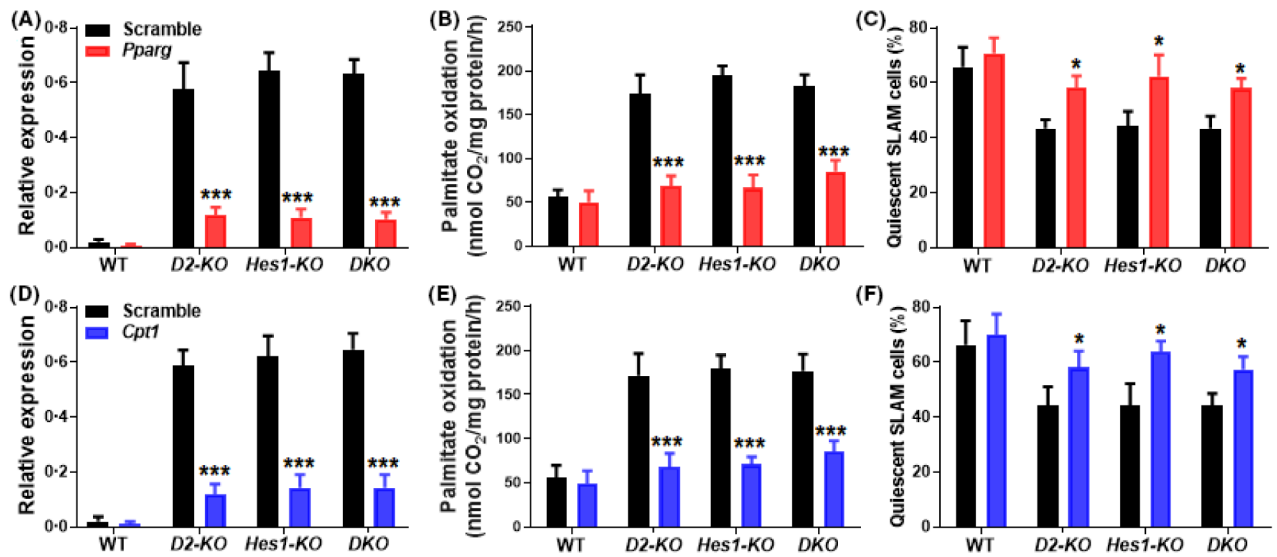


**Fig 6.**

Knockdown of *PPAR<sub>γ</sub>* or *CPT1* reduces fatty-acid oxidation (FAO) and restores quiescence in HSCs deficient for *FANCD2* and *HES1*. (A) Quantitative polymerase chain reaction (qPCR) analysis of *PPAR<sub>γ</sub>* mRNA in shRNA-transduced signaling lymphocyte activation molecule (SLAM) cells Table S1. Bone marrow (BM) Lin<sup>-</sup> cells from WT, *FANCD2*-KO, *HES1*-KO or DKO mice were transduced with an eGFP-lentivirus expressing scramble shRNA or shRNAs targeting *PPAR<sub>γ</sub>*. GFP<sup>+</sup> SLAM cells were treated with TNF-α (10 ng/ml) for 16 h and subjected to qPCR analysis for *PPAR<sub>γ</sub>* expression. Results are means ± standard deviation (SD) of three independent experiments. Comparisons are scramble *versus* sh*PPAR<sub>γ</sub>*. (B) *PPAR<sub>γ</sub>* knockdown reduces inflammation-primed FAO in *FANCD2*-KO haematopoietic stem and progenitor cells (HSPCs). GFP<sup>+</sup> Lin<sup>-</sup> Sca1<sup>+</sup>c-kit<sup>+</sup> (LSK) cells were treated with TNF-α (10 ng/ml) for 16 h, and palmitate oxidation rates were assessed as captured <sup>14</sup>CO<sub>2</sub> using the isolated mitochondria and 1-<sup>14</sup>C-palmitate as substrate. Results are means ± SD of three independent experiments. Comparisons are scramble *versus* sh*PPAR<sub>γ</sub>*. (C) *PPAR<sub>γ</sub>* knockdown restores quiescence in *FANCD2*-KO HSCs. GFP<sup>+</sup> LSK cells in (B) were gated for SLAM population and analyzed for cell-cycle phases by Ki67/Hoechst staining and flow cytometry. Results are means ± SD of three independent experiments. Comparisons are scramble *versus* sh*PPAR<sub>γ</sub>*. (D) qPCR analysis of *CPT1* mRNA in shRNA-transduced SLAM cells. BM Lin<sup>-</sup> cells from WT, *FANCD2*-KO, *HES1*-KO or DKO mice were transduced with an eGFP-lentivirus expressing scramble shRNA or shRNAs targeting *CPT1*. GFP<sup>+</sup> SLAM cells were treated with TNF-α (10 ng/ml) for 16 h and subjected to qPCR analysis for *CPT1*. Results are means ± SD of three independent experiments. Comparisons are scramble *versus* sh*CPT1*. (E) *CPT1* knockdown reduces inflammation-primed FAO in *FANCD2*-KO HSPCs. GFP<sup>+</sup> LSK cells described in (D) were treated with TNF-α (10 ng/ml) for 16 h, and palmitate oxidation rates were assessed as captured <sup>14</sup>CO<sub>2</sub> using the isolated mitochondria and 1-<sup>14</sup>C-palmitate as substrate. Results are means ± SD of three independent experiments. Comparisons are scramble *versus* sh*CPT1*. (F) *CPT1* knockdown restores quiescence in *FANCD2*-KO HSCs. GFP<sup>+</sup> LSK cells in (D) were gated for SLAM population and analyzed for cell-cycle phases by

Ki67/Hocheist staining and flow cytometry. Results are means  $\pm$  *SD* of three independent experiments. Comparisons are scramble *versus* *shCPT1*. \*,  $P < 0.05$ ; \*\*\*,  $P < 0.001$ .

Author Manuscript

Author Manuscript

Author Manuscript

Author Manuscript

Table 1.

Haematopoietic parameters. *P* values were determined using Student's *t* test. WBC count indicates white blood cell count; % Lymphocytes, percentage of WBC count that are lymphocytes; % of Neutrophils, percentage of WBC count that are neutrophils; % of Monocytes, percentage of WBC count that are monocytes; RBC count, red blood cell count; HCT, haematocrit (percentage of whole blood volume); MCV, mean cell volume, Hb, haemoglobin concentration; Plt, platelet count. For all tests on WT, *FANCD2*-KO and *HES1*-KO mice, the sample size was 10. For all tests on double knockout (DKO) mice, the sample size was 9. Comparisons are WT versus single KO or DKO.

WBC count (cells/ul)	Absolute and differential WBC counts				Characterization of red blood cells				Plt (X10 <sup>9</sup> /L)
	% Lymphocytes	% Neutrophils	% Monocytes	RBC count (X10 <sup>12</sup> /L)	HCT, %	MCV, fL	Hb (g/dL)		
WT	7.28±0.69	80.46±4.01	11.16±1.19	2.17±0.49	11.18±1.34	52.1±2.25	54.29±3.25	14.83±1.52	716±83.45
<i>Fancd2</i> -KO	7.15±0.52	69.63±3.94	19.37±1.03	2.93±0.62	10.99±1.29	51.3±2.31	55.37±3.46	15.06±1.47	732±84.06
<i>Hes1</i> -KO	7.42±0.63	75.15±3.35	15.63±1.24	2.44±0.56	11.23±1.42	52.5±2.19	54.46±3.13	13.94±1.52	727±81.94
DKO	7.19±0.48	53.06±4.47	30.39±2.47	3.09±0.78	10.92±1.11	54.32±2.6	51.06±2.32	15.76±1.29	745±85.11
<i>p</i>	.42	.06	.04	.05	.37	.26	.18	.13	.45

**Table II.**

Competitive repopulating units.

<b>Genotype</b>	<b>WT</b>	<b>FANCD2-KO</b>	<b>HES1-KO</b>	<b>DKO</b>
CRU frequency	1/37903	1/67156	1/54274	1/143694

Graded numbers of low-density BM cells from WT, *FANCD2*-KO, *HES1*-KO or double knockout (DKO) mice were transplanted into lethally irradiated recipients. Frequency of competitive repopulating units (CRU) was calculated according to Poisson statistics.  $P = 0.0017$  (WT versus *FANCD2*-KO);  $P = 0.0073$  (WT versus *HES1*-KO);  $P < 0.00010$  (WT versus DKO).

Author Manuscript

Author Manuscript

Author Manuscript

Author Manuscript

Table III.

Competitive repopulating units.

Genotype TNF- $\alpha$	WT		FANCD2-KO		HES1-KO		DKO	
	(-)	(+)	(-)	(+)	(-)	(+)	(-)	(+)
CRU frequency	1/38449	1/46025	1/713101	1/134667	1/507235	1/133118	1/129272	1/146053
<i>P</i>		0.083	0.0021	<0.0001	0.0075	<0.0001	0.0001	<0.0001

Graded numbers of low-density bone marrow (BM) cells from WT, FANCD2-KO, HES1-KO or double knockout (DKO) mice treated with or without TNF- $\alpha$  were transplanted into lethally irradiated recipients. Frequency of competitive repopulating units (CRU) was calculated according to Poisson statistics. Comparisons are WT versus single KO or DKO.



**Table IV.**

Competitive repopulating units.

Genotype Treatment	WT			FANCD2-KO			HES1-KO			DKO		
	V	GW	Eto	V	GW	Eto	V	GW	Eto	V	GW	Eto
CRU frequency	1/46472	1/43030	1/40175	1/134667	1/81126	1/66529	1/137337	1/75185	1/63125	1/146053	1/83558	1/69476
<i>P</i>		0.103	0.087	<0.0001	0.0018	0.0054	<0.0001	0.0041	0.0068	<0.0001	0.0012	0.0059

Graded numbers of TNF- $\alpha$ -primed bone marrow (BM) cells from WT, FANCD2-KO, HES1-KO or double knockout (DKO) mice were treated with vehicle (V), GW9663 (GW) or etomoxir (Eto), and transplanted into lethally irradiated recipients. Frequency of competitive repopulating units (CRU) was calculated according to Poisson statistics. *P* values represent comparison to WT vehicle (V) control. Comparisons are WT *versus* single KO or DKO.